Planar and cagelike structures of gold clusters: Density-functional pseudopotential calculations

Eva M. Fernández*
Departamento de Física Teórica, Atómica y Óptica, Universidad de Valladolid, E-47011 Valladolid, Spain

José M. Soler
Departamento de Física de la Materia Condensada, Universidad Autónoma de Madrid, E-28049 Madrid, Spain

Luis C. Balbás
Departamento de Física Teórica, Atómica y Óptica, Universidad de Valladolid, E-47011 Valladolid, Spain
(Received 1 March 2006; revised manuscript received 5 May 2006; published 28 June 2006)

We study why gold forms planar and cagelike clusters while copper and silver do not. We use density functional theory and norm-conserving pseudopotentials with and without a scalar relativistic component. For the exchange-correlation (xc) functional we use both the generalized gradient (GGA) and the local density (LDA) approximations. We find that planar Au_n structures, with up to $n=11$, have lower energy than the three-dimensional isomers only with scalar-relativistic pseudopotentials and the GGA. In all other calculations, with more than six or seven noble metal atoms, we obtain three-dimensional (3D) structures. However, as a general trend we find that planar structures are more favorable with the GGA than with the LDA. In the total energy balance, kinetic energy favors planar and cage structures, while xc energy favors 3D structures. As a second step, we construct cluster structures having only surface atoms with O_h, T_d, and I_h symmetry. Then, assuming one valence electron per atom, we select those with $2(l+1)^2$ electrons (with l integer), which correspond to the filling of a spherical electronic shell formed by nodeless one-electron wave functions. Using scalar relativistic GGA molecular dynamics at $T=600$ K, we show that the cagelike structures of neutral Au_{32}, Au_{50}, and Au_{162} are metastable. Finally, we calculate the static polarizability of the two lowest-energy isomers of Au_n clusters as a means to discriminate isomers with planar (or cagelike) geometry from those with compact structures. We also fit our data to a semiempirical relation for the size-dependent polarizability which involves the effective valence and kinetic energy components for the homogeneous and inhomogeneous electron densities. Analyzing that fit, we find that the dipole polarizability of gold clusters with planar and cagelike structures corresponds to the linear response of 1.56 delocalized valence electrons, suggesting a strong screening of the valence interactions due to the d electrons.

DOI: 10.1103/PhysRevB.73.235433 PACS number(s): 36.40.Cg, 36.40.Qv

I. INTRODUCTION

Small clusters of metal atoms behave differently than bulk matter, because each additional atom, or even each additional electron, can drastically change their electronic and geometrical properties.[1] Noble metal clusters, with valence electron filling $nd^{10}(n+1)s^1$, differ from the simple s-orbital alkali metals,[2,3] but also present striking differences among Cu, Ag, and Au.[4,5] Well-established structural differences among Au_n^ν ($\nu=0,\pm1$) and Ag_n^ν or Cu_n^ν clusters are the following: (i) Au_n^ν clusters, especially the anions ($\nu=-1$), adopt planar structures up to larger sizes than Ag and Cu clusters, as demonstrated by combined experimental and theoretical studies;[6–9] (ii) experimental photoelectron spectra for noble metal clusters with 55 atoms[10] indicate that silver and copper adopt some symmetry, preferably icosahedral, whereas the pattern for Au_{55} corresponds to an amorphous structure;[11] (iii) anionic and neutral Au_{20} show a tetrahedral T_d geometry,[5,12,13] but Ag_{20} and Cu_{20} have amorphouslike compact C_s structures; (iv) an icosahedral cagelike structure has been found to be very stable for Au_{32},[14,15] but not for silver and copper.[14,16] Other metastable cagelike structures for gold clusters have been proposed recently.[16,17]

The differences between Au and other noble metal clusters are usually attributed to relativistic effects,[4] which stabilize the 6s orbital and destabilize the 5d one, favoring the hybridization of these orbitals. However, although Pt shows as strong relativistic effects as Au,[2] it has been shown that the competition between planar and three-dimensional (3D) structures of Pt clusters is not affected by relativistic effects.[18] Notice that Pt_7 is 3D,[19,20] like Ag_7 or Cu_7, but Au_7 is planar. Notice also that the largest s-orbital contraction due to relativistic effects occurs in Au.[21] Consideration of the spin-orbit coupling does not alter the relative stability of scalar relativistic structures of Au_n clusters with $n\leq20$, but it increases the binding energy by about 0.08 eV/atom (1.85 kcal/mol).[22]

Comparison of density functional theory (DFT) results for Au_6 and Au_8 at several levels of theory (that is, different exchange-correlation functionals) with results from quantum chemical calculations using second-order perturbation theory (MP2) or coupled cluster methods [CCSD(T)] indicate that DFT predicts planar structures, but MP2 and CCSD(T) predict the lowest-energy Au_8 isomer to be nonplanar by 26.6 kcal/mol and 1.5 kcal/mol, respectively.[23] Another recent calculation,[24] using *ab initio* correlated-level theory, predicts Au_8 to be planar.

Concerning DFT calculations, we notice that the type of exchange-correlation (xc) functional has a decisive influence on the structural properties of gold clusters, but it is not so critical for silver and copper clusters.[25] Thus, first-principles

calculations by means of the SIESTA code[26] with scalar relativistic pseudopotentials found planar structures of neutral Au_n clusters with up to six atoms using the local density approximation (LDA) for the xc functional[27] and up to ten atoms using the generalized gradient approximation (GGA).[5] Such a dissimilar result was corroborated by a variety of different pseudopotential and all-electron scalar relativistic DFT calculations using the LDA[28,29] and/or GGA.[29,30]

In a recent paper, Grönbeck and Broqvist[31] compared the different contributions to the binding energy of several planar and 3D structures of Au_8 and Cu_8 clusters, optimized within the GGA and LDA. They found that planar Au_8 isomers have a significantly smaller kinetic energy than 3D ones, which was attributed to *d*-electron delocalization. A correlation between strong *s*-*d* hybridization and high stability of planar structures was found in Ref. 4 for noble metal heptamers, but does not appear to be a general tendency of small Au clusters. Instead, the preference of planar configurations for Au_8 isomers was attributed to a sizable *d*-*d* overlap and to *d*-electron delocalization.[31]

Recently, the σ aromaticity in saturated inorganic rings was examined.[32] Evidence for *d*-orbital aromaticity in square planar noble metal clusters[33] and in triangular gold rings[34] was presented also recently. The spherical π aromaticity of I_h symmetrical gold fullerenes fulfilling a generalized $2(l+1)^2$ *s*-electron rule[35] *et al.*[14] to explain the extra stability of a cagelike Au_{32} cluster with I_h symmetry compared to other space-filling isomers.

A rough estimation of the photoabsorption response of several isomers of Au_{32} and Au_{42} (Ref. 36) suggests that the cagelike structures could be clearly distinguished from space-filling isomers in optical absorption experiments. However, it is difficult to separate in these spectra the spectral features due to symmetry from the features due to empty-cage effects. In this paper we will compare the calculated static dipole polarizability of planar and cagelike Au_n clusters with those for 3D and compact isomers.

In Sec. II, we outline the first-principles method used in our calculations. Results are presented and discussed in Sec. III. In Sec. III A, we compare the GGA and LDA equilibrium structures of Au_n clusters with $6 \leq n \leq 9$. We will focus on the relation of 2D or 3D isomers with the delocalization of *d* electrons, following the ideas of Grönbeck and Broqvist.[31] In Sec. III B we contrast again LDA and GGA predictions for the stability of *magic* cagelike structures Au_{18}, Au_{20}, Au_{32}, Au_{50}, and Au_{160}, compared to amorphouslike filling space isomers. The stability of these cagelike structures against molecular dynamics at constant temperature (600 K) and against the loss or gain of one electron is also tested. In Sec. III C we investigate the use of the calculated static polarizability as a physical property sensible to the cluster structure. In Sec. IV we will present our conclusions.

II. COMPUTATIONAL PROCEDURE

We use the first-principles code SIESTA (Ref. 26) to solve fully self-consistently the standard Kohn-Sham equations[37] of DFT within the GGA as parametrized by Perdew, Burke, and Ernzerhof[38] and within the LDA as parametrized by Perdew and Zunger.[39] For each xc approximation we use a norm-conserving scalar relativistic pseudopotential[40] in its fully nonlocal form,[41] generated from the Au atomic valence configurations $5d^{10}6s^16p^0$, and core radii which we have tested and reported in previous works.[5,42] Flexible linear combinations of numerical (pseudo)atomic orbitals are used as the basis set, allowing for multiple-ζ and polarization orbitals. In order to limit the range of the basis pseudoatomic orbitals (PAO's), they are slightly excited by a common energy shift (0.01 eV in this work) and truncated at the resulting radial node.[43] In the present calculations we used a double-ζ $5p,6s$ basis, with maximum cutoff radius of 7.62 bohrs. The basis functions and the electron density are projected onto a uniform real-space grid in order to calculate the Hartree and exchange-correlation potentials and matrix elements. The grid fineness is controlled by the energy cutoff of the plane waves that can be represented in it without aliasing (120 Ry in this work).

To obtain the equilibrium geometries, an unconstrained conjugate-gradient structural relaxation using the DFT forces[44] was performed for several initial cluster structures (typically more than 10), suggested by the several geometries for Au_n, Au_n^-, and Au_n^+ isomers obtained previously.[5]

The static dipole polarizability of a cluster can be obtained by using the standard numerical finite-field perturbation method, in which the field-dependent energy is expanded with respect to an external uniform electric field $\mathbf{F}$,

$$E = E^0 - \mu_i F_i - \frac{1}{2}\alpha_{ij}F_iF_j - \cdots, \tag{1}$$

where i,j are Cartesian coordinates and the dipole moment and the static dipole polarizability are obtained as energy derivatives, $\mu_i = -\frac{\partial E}{\partial F_i}|_{\mathbf{F}=0}$, and $\alpha_{ij} = -\frac{\partial^2 E}{\partial F_i \partial F_j}|_{\mathbf{F}=0}$, respectively. The external electric-field values used in our calculations were (in a.u.) $|\mathbf{F}| = 0.000$, 0.001, 0.006, 0.010, 0.014, and 0.018. The energies calculated for these values were fitted to a polynomial expansion to obtain the first-order and second-order derivatives of energies with respect to the electric-field strength. The mean polarizability is calculated as $\bar{\alpha} = \mathrm{Tr}(\alpha_{ij})/3$.

III. RESULTS AND DISCUSSIONS

A. Planarity and *d*-electron delocalization in Au_n

The onset of three-dimensional structures of neutral Au_n clusters was calculated at $n=11$ within the GGA (Ref. 5) and at $n=7$ within the LDA (Ref. 27). In this work we compare the planar and 3D lowest-energy isomers of Au_n ($6 \leq n \leq 9$) calculated within the SIESTA code[26] and using the LDA (Ref. 39) and GGA (Ref. 38) for xc functionals (with the corresponding LDA and GGA scalar relativistic pseudopotentials). Figure 1 shows our results for the geometry of these isomers. The lower-energy isomer is the planar one for the GGA and the 3D one for the LDA, except for $n=6$. Table I gives the binding energy difference between 2D and 3D isomers, $\Delta E_b = E_b(Au_n) - E_b(Au_n^*)$, for the relativistic and nonrelativistic calculations. We see that the GGA leads to planar structures, but the LDA favors 3D structures for $n \geq 7$ clusters.

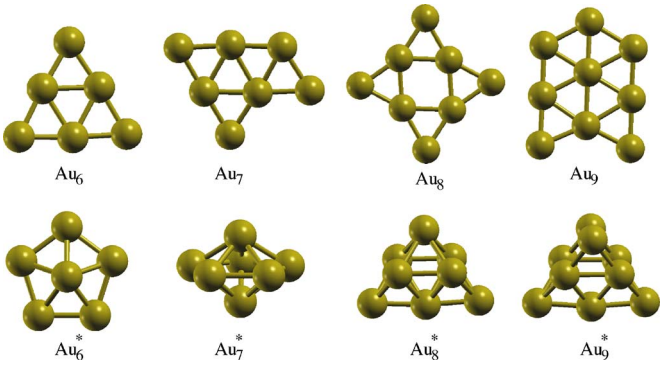

FIG. 1. (Color online) Equilibrium geometry of the lowest-energy isomers of gold clusters having planar (Au_n, upper row) or three-dimensional (Au_n^*, lower row) geometry as resulting from LDA and GGA scalar relativistic calculations. For GGA the ground state is the planar Au_n isomer. For the LDA the ground state is the 3D Au_n^* isomer, except for $n = 6$, whose structure is also the planar Au_6.

Thus, although the planarity of Au_7 compared to the 3D structures of Ag_7 or Cu_7 was attributed to relativistic effects,[4] the observed planarity of Au clusters[6–8] is accounted for only using the GGA theory. We have also optimized the Au_n structures in Fig. 1 within GGA and LDA nonrelativistic pseudopotentials, resulting in the 3D structures becoming more stable energetically than the planar ones, except for $n=6$ within the GGA, as shown in the last row of Table I.

Table II gives the various energy differences (total, kinetic, Coulomb, and exchange correlation) between the second and first energy isomers of scalar relativistic Au and Cu clusters with $6 \leq n \leq 9$ atoms. We will denote compact 3D structures with an asterisk, while its absence indicates planar and cagelike geometries. The geometry of the Au isomers is given in Fig. 1. The geometries of Cu_6 and Cu_6^* are similar to those of Au_6 and Au_6^*, respectively. For Cu_n with $n=7$, 8, 9, the geometries of the two lowest-energy isomers are both 3D and are taken from our previous work.[5] We can see in Table II that planar structures have smaller kinetic energy than 3D isomers and larger for the LDA than for the GGA. Adding kinetic and Coulomb energies, the 2D structures became more stable energetically than the 3D ones. On the other hand, the xc energy is more negative (it contributes more to the binding energy) for 3D than for planar structures. Both effects are stronger within the LDA, but in the balance of total energy difference, the loss of kinetic energy in planar structures dominates over the increase of xc energy when using the GGA, but the opposite occurs with the LDA. Thus, as a whole, the GGA (LDA) favors 2D (3D) structures of gold clusters. On the other hand, for Cu_6 and Cu_6^* isomers, which have the same geometry as Au_6 and Au_6^*, the change in kinetic and Coulomb energies is not so noticeable as in gold.

TABLE I. The binding energy difference $\Delta E_b = E_b(Au_n) - E_b(Au_n^*)$, in eV, between the 2D and 3D isomers of the gold clusters represented in Fig. 1, optimized within LDA and GGA xc functionals using relativistic and nonrelativistic (NR) pseudopotentials.

	Au_6		Au_7		Au_8		Au_9	
	LDA	GGA	LDA	GGA	LDA	GGA	LDA	GGA
ΔE_b	0.14	0.15	−0.02	0.03	−0.06	0.01	−0.04	0.01
ΔE_b^{NR}	−0.04	0.02	−1.42	−1.11	−1.64	−1.37	−1.29	−0.98

For Cu_n with $n=7-9$, whose first and second isomer geometries are all 3D, the change in exchange-correlation energy, Δ_{xc}, can be positive or negative. For Cu_8, whose electronic properties can be described approximately by the spherical jellium model,[5] we see that the sum of changes in kinetic and Coulomb energies roughly cancel each other, resulting that the change in the total energy is ruled by the change in xc energy, as in the jellium model.[45]

The loss of kinetic energy in planar gold clusters with respect to their 3D isomers was attributed to electron delocalization,[31] but it is not easy to reconcile that delocalization with the simultaneous confinement in two dimensions. On the other hand, the xc energy becomes less negative for planar configurations, which is also not clearly related to delocalization and confinement in 2D gold clusters. We observe that the calculated average bond length d_{av} is larger for 3D than for 2D isomers. Specifically, the difference between d_{av} of 3D and 2D Au_n isomers with $n=6$, 7, 8, 9 is

TABLE II. Total, kinetic, Coulomb, and exchange-correlation energy differences $[\Delta E_i = E_i(Au_n^*) - E_i(Au_n)]$, in eV, between the second isomer (3D, Au_n^*) and first isomer (2D, Au_n) of gold clusters with the structures of Fig. 1. For Cu_n the first and second isomers are 3D, except for Cu_6, where the two isomers are similar to Au_6 and Au_6^*. The Cu_n geometries are taken from Ref. 5.

	ΔE_{tot}		ΔE_{kin}		ΔE_{Coul}		ΔE_{xc}	
	LDA	GGA	LDA	GGA	LDA	GGA	LDA	GGA
Au_6	0.86	0.88	11.01	10.63	−9.62	−9.42	−0.53	−0.33
Au_7	−0.15	0.24	12.49	10.34	−11.12	−9.52	−1.53	−0.57
Au_8	−0.46	0.04	7.37	7.03	−6.53	−6.80	−1.30	−0.19
Au_9	−0.34	0.07	5.07	4.63	−4.50	−4.52	−0.91	−0.04
Cu_6		0.03		1.03		−0.78		−0.22
Cu_7		0.34		0.20		−0.98		1.13
Cu_8		0.89		2.10		−1.98		0.77
Cu_9		0.25		−1.60		1.87		−0.02

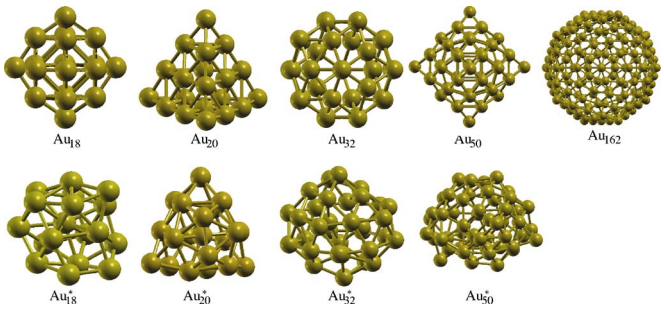

FIG. 2. (Color online) Cagelike (Au_n) and space-filling (Au_n^*) equilibrium isomeric structures of neutral gold clusters with $n=18$, 20, 32, 50, and 162, except Au_{162}^* which is not optimized in this paper.

(in Å) 0.04, 0.11, 0.13, 0.09 (0.05, 0.11, 0.09, 0.09) for the LDA (GGA) calculation.

The kinetic energy of the electron gas in two dimensions is about one-half of the 3D case at the same density parameter r_s, while the exchange energy in 2D is slightly larger than in 3D.[46,47] However, the correlation energy, at least in the random phase approximation (RPA), is much larger in 2D than in 3D.[46] This consideration points again to the importance of good exchange-correlation functionals in dealing with the DFT structural description of gold clusters.

B. Magic cagelike structures of gold clusters

Stable cagelike structures of gold clusters have been predicted recently for Au_{32},[14,15] Au_{26},[48] Au_{42},[49] and others.[16,17] On the other hand, although all atoms of Au_{20} are at the surface, this cluster can be considered as a small piece of bulk fcc gold.[5,12,13]

In this work we construct cagelike atomic structures starting with the Platonic solids with triangular faces—tetrahedron (T_d), octahedron (O_h), and icosahedron (I_h)—which are those allowing compact planar packing. By adding atoms at the intersections of fcc planes in the triangles, we obtain the following sequences for the number of atoms: $n(T_d)=4+2m(m+2)$, $n(O_h)=6+4m(m+2)$, and $n(I_h)=12+10m(m+2)$, where $m=0,1,2,\ldots$ is the number of atoms inserted in each edge. When we add a central atom to each new triangle, we obtain cagelike structures with $n(T_d)=2+6(m+1)^2$, $n(O_h)=2+12(m+1)^2$, and $n(I_h)=2+30(n+1)^2$. On the other hand, from the electronic point of view, a cluster with nearly free valence electrons is magic when it has filled electronic shells, having well-defined angular momentum, as in the jellium model. As we look for an empty cage with an approximately spherical surface, orbitals with radial nodes have to be excluded and the only allowed electronic shells are $1s,1p,1d,1f,\ldots$. This leads to a magic number of electrons $n_e=2(l+1)^2$, where l is an integer number.[50] Assuming that each noble metal atom contributes with one valence electron, the equality $n=2(l+1)^2$ leads to the following magic neutral cagelike Au_n clusters (containing less than 1000 atoms): $n=8$ (T_d), 18 (O_h), 32 (I_h), 50 (O_h), 98 (T_d), 162 (I_h), and 578 (O_h). Double anionic clusters should obey $n+2=2(l+1)^2$, and they appear at $n=6$ and 198 (O_h) atoms. Double cationic magic clusters are the solutions of $n-2=2(l+1)^2$. However, we exclude the T_d clusters because they are far from spherical. Also Au_{20} cannot be properly considered cage like because it contains many internal bonds, as similarly occurs to smaller clusters, like Au_{18}. Nevertheless, in the following we will test the estructural and electronic properties of Au_n clusters with 18, 20, 32, 50, and 162 atoms.

TABLE III. Binding energy difference between the cagelike and compact structures of Fig. 2, $\Delta E_b=E_b(Au_n)-E_b(Au_n^*)$, optimized with the LDA and GGA.

	Au_{18}		Au_{20}		Au_{32}		Au_{50}	
	LDA	GGA	LDA	GGA	LDA	GGA	LDA	GGA
ΔE_b	−0.07	0.01	0.01	0.03	−0.06	0.01	−0.14	0.01

We performed full relaxations of the initial cagelike magic structures and several compact geometries obtained by forcing initially some surface atoms inside these clusters. Figure 2 shows the equilibrium geometries with cagelike and compact structures, obtained after a nonexhaustive search and optimized with forces ≤ 0.01 eV/Å at the GGA and LDA levels. The cagelike equilibrium structures were proven to be metastable after performing an *ab initio* molecular dynamics run at temperature of 600 K during 1000 steps, each of 2 fs. The binding energy difference between cagelike and compact structures is tabulated in Table III. We see that cagelike GGA structures are slightly more bound than the compact ones. Instead, the LDA leads to compact structures without symmetry, except for Au_{20}. The true ground state is not known, however, and improved functionals could lead to compact, ordered or disordered, structures.

As a further test, we calculate the relative stability of cagelike and compact isomers after loss or gain of one electron. Figure 3 shows the total energy difference per atom between cagelike and compact equilibrium structures of cationic, neutral, and anionic clusters with $n=18$, 20, 32 atoms. We see that only the cation Au_{32}^+ and the anion Au_{20}^- are still cage like. Interestingly, the lowest-energy isomer of both ionic clusters Au_{18}^+ and Au_{18}^-, is not cage like, contrary to the neutral Au_{18}.

In Fig. 4 we compare the density of states (DOS) of the cagelike and amorphous structures of neutral Au_n (n

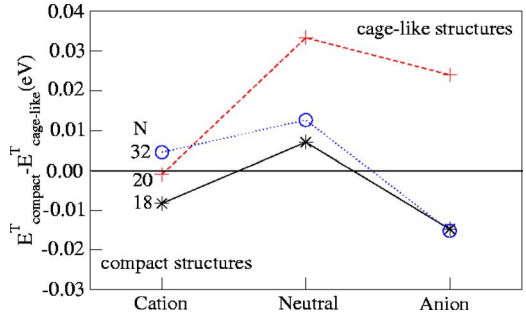

FIG. 3. (Color online) Total GGA energy difference per atom (in eV) between the lower-energy isomer of compact and cagelike structures for cationic, neutral, and anionic clusters of gold with $n=18$ (stars), 20 (crosses), and 32 (circles) atoms.

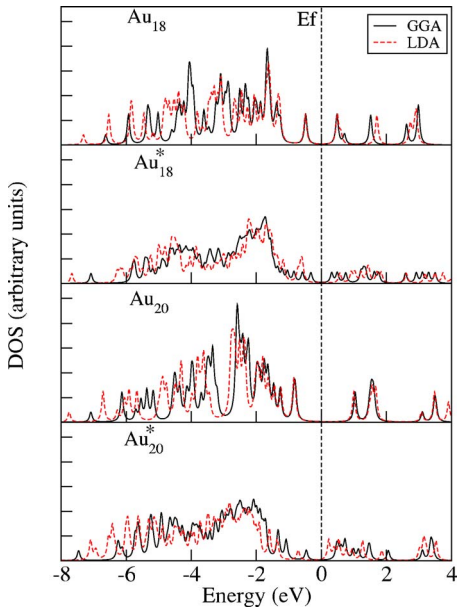

FIG. 4. (Color online) Density of states (DOS) of the lower-energy cagelike and amorphous isomers of Au clusters with 18 and 20 atoms, calculated at the LDA and GGA levels of theory.

=18,20). We see that the cagelike geometries show a more structured DOS, with well-defined peaks. This is probably due to a higher geometrical symmetry (O_h for Au_{18} and T_d for Au_{20}), as shown in a previous work for Au_{55}.[10] This fact is independent of the GGA or LDA level of theory. The LDA DOS profile tends to be shifted (to lower energies for Au_{20}) with respect to the GGA one, and the highest occupied and lowest unoccupied molecular orbital (HOMO-LUMO) gap is smaller for the LDA than for the GGA. On the other hand, the HOMO-LUMO gap is considerably larger for cagelike Au_{20} than for cagelike Au_{18}, indicating that the former is much more stable than the latter.

C. Static dipole polarizability

The minimum polarizability principle states that any system evolves naturally towards a state of minimum polarizability, but exceptions have been reported.[51] In Table IV are given the results of our scalar-relativistic GGA calculations for the mean polarizability per atom of the two lowest-energy states of the Au clusters reported in the subsections above.

The static dipole polarizability of atomic Au comes to 20.53 a.u. (bohr^3) for the scalar-relativistic calculation and 33.06 a.u. for the nonrelativistic calculation, which is a clear manifestation of the relativistic size contraction of gold.[2] Our Au polarizability is smaller than other calculated and experimental values quoted in the literature.[2,52–54] Different estimates of the experimental value are 30±4 a.u. (Ref. 2) and 39.1±9.8 a.u. (Ref. 52). A quantum chemical CCSD(T) calculation gives 36.06 a.u. (Ref. 53), and a recent CASSCF-CASPT2 relativistic calculation gives 27.9 a.u. (Ref. 52).

For noble metal dimers, recent relativistic and nonrelativistic calculations[55] found that the reduction of the polarizability, due to the relativistic contraction effect, amounts to

TABLE IV. The third and fourth columns give, respectively, the mean polarizability per atom $\bar{\alpha}/n$ of the first and second isomers of Au_n clusters. The last column gives their difference. For comparison, the first column gives the $\bar{\alpha}$/n value calculated by Zhao and co-workers for planar structures (Ref. 57). All polarizabilities are in atomic units (bohr^3).

n	Ref. 57	$\bar{\alpha}/n$ First isomer	$\bar{\alpha}/n$ Second isomer	$\Delta\bar{\alpha}$(%)
2	29.4	28.3	29.0	2.5
3	31.1	36.4	43.0	18.2
4	32.7	31.5	37.2	17.9
5	34.2	32.9	46.6	41.6
6	34.2	32.7	40.0	22.5
7	34.3	33.9	30.9	−9.0
8	36.2	34.7	36.1	4.2
9	38.5	37.8	48.1	27.3
18	42.7	32.1	31.4	−2.4
20	43.7	35.2	32.9	−6.4
32		33.9	33.5	−1.3

39.8% for Au_2, 15.8% for Ag_2, and 6% for Cu_2. From the time-dependent (TDDFT) study of Castro,[54] the static polarizability of Au_n clusters up to $n=4$ are affected up to ~2% by the inclusion of the spin-orbit term.

From the TDDFT calculations of Castro *et al.*,[56] the static polarizability of the 3D tetrahedral isomer of Au_4 is 2.5% higher than the one for the planar D_{2h} ground state. We obtain a larger difference (15.5%) between our two planar Au_4 isomers (a rhombus and a triangle with another Au on top; see Ref. 5). Our result for the Au_n polarizability with $n=2-9$, is similar to the one calculated by Zhao and co-workers[57] using a finite-field perturbation method like ours. However, the polarizability per atom obtained by these authors for planar Au_{18} and Au_{20} is much higher than ours for cagelike and compact isomers. On the other hand, the difference between the GGA and LDA polarizabilities of planar Au_n clusters ($n=2-20$) calculated in Ref. 57 is less than 2%.

We see in Table IV that the average polarizability per atom of Au_n clusters is remarkably constant, with small odd-even effects for $n\leq 7$. Up to $n=6$ the first and second isomers are planar, and the larger polarizability of the second isomer is due to the larger average Au-Au bond length. The polarizability of the Au_7^* 3D isomer is smaller than that of the planar isomer, due to the compact pentagonal bipyramid geometry, and it constitutes one of the exceptions to the minimum polarizability principle.[51] The cagelike structures seem to be another exception to that rule.

The average mean polarizability per atom for the first isomer of Au_n clusters in Table IV is $\bar{\alpha}_{av}/n=33.57$ a.u. The jellium model for atomic clusters of monovalent metals fulfills the relation $\alpha_{jel}=r_s^3 n$, where r_s is the radius per electron (in a.u.) of the bulk metal. For Au, with $r_s=3.01$ and the GGA, we obtain the ratio $\tilde{\alpha}\equiv\bar{\alpha}_{av}/\alpha_{jel}=1.23$. We can calculate a similar ratio for Li, Na, Cu, and Ag clusters using results from experiments and other calculations. Using the

experimental values[58,59] for the dipole polarizability of Li (r_s=3.25), Na (r_s=3.93), and Cu (r_s=2.67) clusters with $n \leq 10$, we obtain the ratios $\tilde{\alpha}_{expt}$(Li)=2.26, $\tilde{\alpha}_{expt}$(Na)=2.11, and $\tilde{\alpha}_{expt}$(Li)=2.0 for Li, Na, and Cu, respectively. From the GGA polarizability values calculated in Ref. 60 for Li and Na clusters with $n \leq 10$, we find $\tilde{\alpha}_{GGA}$(Li)=2.47 and $\tilde{\alpha}_{GGA}$(Na)=1.81. For Cu clusters in the same range of sizes, using the different GGA and LDA polarizability values reported by Yang and Jackson,[61] one has $\tilde{\alpha}_{GGA}$(Cu) =1.93–1.98 and $\tilde{\alpha}_{LDA}$(Cu)=1.79. Using recent calculations[17] for the polarizability of Ag clusters with $2 \leq n \leq 8$ results in $\tilde{\alpha}_{GGA}$(Ag)=1.69. As a whole, we see that the ratio $\bar{\alpha}_{av}/\alpha_{jel}$ is considerably smaller for Au than for Li, Na, Cu, and Ag clusters.

The enhancement of dipole polarizability over the classical jellium model (Mie value α_{jel}) is directly proportional to the fraction of electronic charge that extends beyond the positive background in the field-free system (spill-out).[1] The smaller spill-out for gold with respect to silver and copper can be attributed tentatively to the relativistic contraction of the electronic cloud.[2,21]

We can explore a little more our calculated polarizability values using an extended Thomas-Fermi-Weizsäcker (TFλW) jellium model,[62] which predicts the mean polarizability of a cluster with $n_e=vn$ valence electrons (v =valence, n =number of atoms) as

$$\bar{\alpha} = \alpha_{jel}\left[1 + 3\frac{d(r_s)}{r_s} n_e^{-1/3}\left(1 + \frac{\alpha_1(r_s)}{\alpha_0(r_s)} n_e^{-1/3}\right)\right]. \qquad (2)$$

In this expression, $d(r_s)$ is the image plane position (the centroid of the induced electron density for the flat metal surface), and α_1 and α_0 are two coefficients dependent on the parameter λ, which take into account the weight of the inhomogeneity-density correction (Weizsäcker term) to the Thomas-Fermi kinetic energy. In the interval $3 \leq r_s \leq 4$, it results in $\alpha_1(r_s) \simeq -0.1$ a.u. independently of the λ value (see Fig. 1 of Ref. 62), but $\alpha_0(r_s)$ is strongly dependent on λ. In terms of a reduced polarizability, defined by $\alpha_{red}=(\bar{\alpha}/\alpha_{jel} -1)n^{2/3}$, we can write Eq. (2) as

$$\alpha_{red} = An^{1/3} + AB, \qquad (3)$$

where $A=\frac{3}{v^{1/3}}\frac{d(r_s)}{r_s}$ and $B=\frac{1}{v^{2/3}}\frac{\alpha_1(r_s)}{\alpha_0(r_s)}$. By fitting our data in Table IV to Eq. (3), we obtain $\alpha_{red}=1.15n^{1/3}-1.26$, and using d(Au)=1.34 a.u. for the image plane distance of gold,[63] there results an effective valence $v=1.56$ and a ratio $\frac{\alpha_1(r_s)}{\alpha_0(r_s)}$ $=-1.46$. For $\alpha_1(\mathrm{Au}) \simeq -0.1$ we obtain α_0(Au)=0.07. Extrapolating the results in Fig. 1 of Ref. 62, such a small α_0(Au) value corresponds to an extremely small value of the parameter λ, which means that the contribution of inhomogeneity corrections to the kinetic energy is very small. This result agrees with our conclusion in Sec. III A about the delocalization of valence electrons in planar gold clusters. On the other hand, the effective valence $v=1.56$ reflects in some way the screening of the dipole response due to the d electrons.[56]

We test also an empirical linear relation between the cubic root of the mean polarizability per atom, $\bar{\alpha}^{1/3}/n$, and the inverse of the ionization potential per atom, I_p^{-1}/n. That relation was tested in Ref. 60 for Li and Na clusters with two to ten atoms, resulting for both cases (using calculated GGA values, in a.u.) in a proportionality constant close to unity, with a linear correlation coefficient 0.995. For the lower-energy isomers of Au clusters reported in Table IV, there results a proportionality constant of 0.925 and a correlation coefficient of 0.984.

As probed by Yang and Jackson,[61] temperature effects are a possible source of discrepancy between calculated and measured polarizabilities, because calculations are carried out for 0 K while experiments are conducted at finite temperatures. The existence of a permanent electric dipole in a cluster adds the following temperature-dependent term to the effective polarizability:[64]

$$\alpha_{eff} = \bar{\alpha} + \frac{\mu^2}{3kT}, \qquad (4)$$

where μ is the dipole moment and k is Boltzman's constant. The dipole contribution is important at low temperatures for clusters with permanent dipole moments. Using the dipole moments calculated for our GGA lower-energy isomers, the correction of Eq. (4) to the mean polarizability per atom at $T=2$ K is (in a.u.) 1.39, 0.04, 0.74, 2.33, and 0.09, for clusters with 3, 4, 5, 6, and 20 atoms, respectively. This small correction still allows one to discriminate the polarizability of planar and cagelike gold clusters from their isomers.

IV. CONCLUSIONS

We obtain that, using nonrelativistic pseudopotentials, both the GGA and LDA predict the onset of three-dimensional cluster structures already at $n=6$ for Cu_n and Ag_n and at $n=7$ (6) for Au_n. This result changes by considering scalar-relativistic pseudopotentials within the GGA, resulting in planar Au_n structures up to $n=11$.

From our scalar-relativistic results for the two lowest-energy isomers of Au_n and Cu_n with $n=6-9$ atoms, we find that planar structures have smaller kinetic energy than 3D isomers, and this effect is much larger for gold than for copper clusters. Adding kinetic and Coulomb energies, the 2D structures became more stable than the 3D ones, and this effect is more noticeable for the LDA than for the GGA. On the other hand, the xc energy is more negative (contributes more to the binding energy) for 3D than for planar structures, and this effect is notably enhanced within the LDA. Thus, in the total energy balance, kinetic energy loss favors planar GGA structures, but xc energy favors LDA 3D structures.

As a second step, we constructed clusters having only surface atoms, and with O_h, T_d, and I_h symmetry. From those, assuming one valence electron per atom, we select the ones having $2(l+1)^2$ electrons, which correspond to the filling of a spherical electronic shell formed by nodeless one-electron wave functions. We obtain, by means of scalar-relativistic GGA calculations, that these cagelike structures for neutral Au_{18}, Au_{20}, Au_{32}, Au_{50}, and Au_{162} are metastable

after moderate (600 K) constant-temperature molecular dynamics. However, after the addition or substraction of an electron, only the anion Au_{20}^- and the cation Au_{32}^+ remain cage like.

Finally, we calculate the static polarizability of the two lowest-energy isomers of Au_n clusters, which are planar ($n=2-9$) and cage like ($n=18,20,32$) for the first isomer and planar ($n=2-6$) or space filling 3D ($n=7-9,18,20,32$) for the second isomer. In the range $n=2-9$, the polarizability per atom is smaller for the first isomer than for the second, with the exception of $n=7$, confirming the empirical rule of minimum polarizability. The contrary occurs for cagelike structures, with larger $\bar{\alpha}$ than their space-filling isomers.

We fitted the polarizability of the first isomer of these gold clusters to a semiempirical relation between the cluster dipole polarizability and its size, which involves the effective atomic valence and the kinetic energy due to homogeneous and to inhomogeneous density components. From that fit we extract a very small value for the kinetic energy component due to inhomogeneous density, which suggests a delocalized character of the valence electrons involved in the dipole response. We also obtain an effective valence charge of 1.56 electrons, reflecting a dipole response with strong screening of the *d* electrons, as already reported previously.[56]

ACKNOWLEDGMENTS

We want to acknowledge the financial support from Grants Nos. MAT2005-03415 and BFM2003-03372 of the Spanish Ministry of Science and from the FEDER of the European Community.

*Electronic address: efernand@fta.uva.es

[1] W. Ekardt, *Metal Clusters* (Wiley, Chichester, 1999).
[2] P. Pyykkö, Angew. Chem., Int. Ed. **43**, 4412 (2004).
[3] P. Pyykkö, Inorg. Chim. Acta **358**, 4113 (2005).
[4] H. Häkkinen, M. Moseler, and U. Landman, Phys. Rev. Lett. **89**, 033401 (2002).
[5] E. M. Fernández, J. M. Soler, I. L. Garzón, and L. C. Balbás, Phys. Rev. B **70**, 165403 (2004).
[6] F. Furche, R. Ahlrich, P. Weis, C. Jacob, S. Gilb, T. Bienweiler, and M. Kappes, J. Chem. Phys. **117**, 6982 (2002).
[7] P. W. S. Gilb, F. Furche, R. Ahlrichs, and M. M. Kappes, J. Chem. Phys. **116**, 4094 (2002).
[8] P. Weis, T. Bierweiler, S. Gilb, and M. M. Kappes, Chem. Phys. Lett. **355**, 355 (2002).
[9] H. Häkkinen, B. Yoon, U. Landman, X. Li, H.-J. Zhai, and L.-S. Wang, J. Phys. Chem. A **107**, 6168 (2003).
[10] H. Häkkinen, M. Moseler, O. Kostko, N. Morgner, M. A. Hoffmann, and B. von Issendorff, Phys. Rev. Lett. **93**, 093401 (2004).
[11] I. L. Garzón, K. Michaelian, M. R. Beltrán, A. Posada-Amarillas, P. Ordejón, E. Artacho, D. Sánchez-Portal, and J. M. Soler, Phys. Rev. Lett. **81**, 1600 (1998).
[12] J. Li, X. Li, H.-J. Zhai, and L.-S. Wang, Science **299**, 864 (2003).
[13] J. Wang, G. Wang, and J. Zhao, Chem. Phys. Lett. **380**, 716 (2003).
[14] M. P. Johansson, D. Sundholm, and J. Vaara, Angew. Chem., Int. Ed. **43**, 2678 (2004).
[15] X. Gu, M. Ji, S. H. Wei, and X. G. Gong, Phys. Rev. B **70**, 205401 (2004).
[16] E. Fernández, M. B. Torres, and L. C. Balbás, Prog. Theor. Phys. **15**, 407 (2006).
[17] J. Wang, J. Jellinek, J. Zhao, Z. Chen, R. B. King, and P. v. R. Schleyer, J. Phys. Chem. A **109**, 9265 (2005).
[18] L. Xiao and L. Wang, J. Phys. Chem. A **108**, 8605 (2004).
[19] W. Q. Tian, M. Ge, B. R. Sahu, D. Wang, T. Yamada, and S. Mashiko, J. Phys. Chem. A **108**, 3806 (2004).
[20] W. Q. Tian, M. Ge, B. R. Sahu, D. Wang, T. Yamada, and S. Mashiko, J. Phys. Chem. A **109**, 6620 (2005).
[21] P. Schwerdtfeger, Heteroat. Chem. **13** (2002).
[22] L. Xiao and L. Wang, Chem. Phys. Lett. **392**, 452 (2004).
[23] R. M. Olson, S. Varganov, M. S. Gordon, H. Metiu, S. Chretien, P. Piecuch, K. Kowalski, S. Kucharski, and M. Musial, J. Am. Chem. Soc. **127**, 1049 (2005).
[24] V. K. Han, J. Chem. Phys. **124**, 024316 (2006).
[25] C. Massobrio, A. Pasquarello, and A. D. Corso, J. Chem. Phys. **109**, 6626 (1998).
[26] J. M. Soler, E. Artacho, J. D. Gale, A. García, P. O. J. Junquera, and D. Sánchez-Portal, J. Phys.: Condens. Matter **14**, 2745 (2002).
[27] B. S. de Bas, M. J. Ford, and M. B. Cortie, J. Mol. Struct.: THEOCHEM **686**, 193 (2004).
[28] J. Wang, G. Wang, and J. Zhao, Phys. Rev. B **66**, 035418 (2002).
[29] A. V. Walker, J. Chem. Phys. **122**, 094310 (2005).
[30] F. Remacle and E. S. Kryachko, J. Chem. Phys. **122**, 044304 (2005).
[31] H. Grönbeck and P. Broqvist, Phys. Rev. B **71**, 073408 (2005).
[32] Z.-H. Li, D. Moran, K.-N. Fan, and P. v. R. Schleyer, J. Phys. Chem. A **109**, 3711 (2005).
[33] C. S. Wannere, C. Corminboeuf, Z.-X. Wang, M. D. Wodrich, R. B. King, and P. von R. Schleyer, J. Am. Chem. Soc. **127**, 5701 (2005).
[34] A. C. Tsipis and C. A. Tsipis, J. Am. Chem. Soc. **127**, 10623 (2005).
[35] A. Hirsch, Z. Chen, and H. Jiao, Angew. Chem., Int. Ed. **39**, 3915 (2000).
[36] W. Fa, C. Luo, and J. Dong, Phys. Rev. B **73**, 085405 (2006).
[37] W. Kohn and L. J. Sham, Phys. Rev. **145**, 561 (1965).
[38] J. P. Perdew, K. Burke, and M. Ernzerhof, Phys. Rev. Lett. **77**, 3865 (1996).
[39] J. P. Perdew and A. Zunger, Phys. Rev. B **23**, 5048 (1981).
[40] N. Troullier and J. L. Martíns, Phys. Rev. B **43**, 1993 (1991).
[41] L. Kleinman and D. M. Bylander, Phys. Rev. Lett. **48**, 1425 (1982).
[42] E. M. Fernández, M. B. Torres, and L. C. Balbás, Int. J. Quantum Chem. **99**, 39 (2004).
[43] O. F. Sankey and D. J. Niklewski, Phys. Rev. B **40**, 3979 (1989).
[44] L. C. Balbás, J. L. Martíns, and J. M. Soler, Phys. Rev. B **64**, 165110 (2001).

[45] A. Rubio, L. C. Balbás, and J. A. Alonso, Z. Phys. D: At., Mol. Clusters **26**, 284 (1993).
[46] E. Lipparini, *Modern Many-Particle Physics* (World Scientific, Singapore, 2003), p. 51.
[47] M. L. Glasser and J. Boersma, SIAM J. Appl. Math. **43**, 535 (1983).
[48] W. Fa, C. Luo, and J. Dong, Phys. Rev. B **72**, 205428 (2005).
[49] Y. Gao and X. C. Zeng, J. Am. Chem. Soc. **127**, 3698 (2005).
[50] Formally, this number of electrons is identical to the one allowed by the spherical aromaticity rule to constitute fullerenes (Ref. 35).
[51] M. Torrent-Sucarrat, M. Duran, J. M. Luis, and M. Solá, J. Phys. Chem. A **109**, 615 (2005).
[52] B. O. Roos, R. Lindh, P.-A. Malmqvist, V. Veryazov, and P.-O. Widmark, J. Phys. Chem. **109**, 6575 (2005).
[53] P. Neogrady, V. Kello, M. Urban, and A. J. Sadlej, Int. J. Quantum Chem. **63**, 557 (1997).
[54] A. Castro, Ph.D. thesis, Universidad de Valladolid, Spain, 2004.
[55] T. Saue and H. J. A. Jensen, J. Chem. Phys. **118**, 522 (2003).
[56] A. Castro, M. A. L. Marques, J. A. Alonso, and A. Rubio, J. Comput. Theor. Nanosci. **1**, 231 (2004).
[57] J. Zhao, J. Yang, and J. G. Hou, Phys. Rev. B **67**, 085404 (2003).
[58] E. Benichou *et al.*, Phys. Rev. A **59**, R1 (1999).
[59] D. Rayane *et al.*, Eur. Phys. J. D **9**, 243 (1999).
[60] K. R. S. Chandrakumar, T. K. Ghanty, and S. K. Ghosh, J. Phys. Chem. A **108**, 6661 (2004).
[61] M. Yang and K. A. Jackson, J. Chem. Phys. **122**, 184317 (2005).
[62] A. Mañanes, M. Membrado, A. F. Pacheco, J. Sañudo, and L. C. Balbás, Int. J. Quantum Chem. **52**, 767 (1994).
[63] J. P. Perdew, Phys. Rev. B **37**, 6175 (1988).
[64] I. Vasiliev, S. Öğüt, and J. R. Chelikowsky, Phys. Rev. Lett. **78**, 4805 (1997).